Available online at www.sciencedirect.com
ScienceDirect
Dyes and Pigments 76 (2008) 760–764
DYES and PIGMENTS
www.elsevier.com/locate/dyepig

The electronic structure of C.I. Pigment Red 209

Takatoshi Senju*, Jin Mizuguchi

Department of Applied Physics, Graduate School of Engineering, Yokohama National University, 79-5 Tokiwadai, Hodogaya-ku, 240-8501 Yokohama, Japan

Received 1 November 2006; received in revised form 29 January 2007; accepted 31 January 2007
Available online 16 February 2007

Abstract

C.I. Pigment Red 209 (PR209) is a mixture of three kinds of isomeric dichloroquinacridones, 3,10-, 1,8-, and 1,10-derivatives. The colorant has attracted attention for its yellow shade of red, which is unusual for a quinacridone pigment. Elucidation of the pigment's crystal structure revealed that, of the three derivatives, only 3,10-DClQA was isolated as single crystals. X-ray analysis showed that 3,10-DClQA crystallizes in $P\bar{1}$ space group and that NH···O intermolecular hydrogen bonds in the $[1\bar{1}0]$ direction and which constitute a two-dimensional, hydrogen bond network. However, whilst 3,10-DClQA was found to lack the yellowish hue of PR209, the color can be attributed to 1,8- and 1,10-DClQAs which possess absorption bands at shorter wavelengths than 3,10-DClQA.

Keywords: C.I. Pigment Red 209; 3,10-Dichloroquinacridone; Crystal structure; Hydrogen-bonded pigment

1. Introduction

Quinacridones (QAs) are industrially important hydrogen-bonded red pigments [1] that exhibit a wide range of red hues, varying from vivid red to bluish red, depending upon their crystal phases. Of these, C.I. Pigment Red 209 (abbreviated as PR209) has stimulated much interest because of its yellowish red shade, which is unusual for a QA pigment. PR209 is a mixture of three kinds of isomeric dichloroquinacridones that are formed during its synthesis namely, 3,10-, 1,8-, and 1,10-derivatives (Figs. 1 and 2) [2] of which, 3,10-dichloroquinacridone (3,10-DClQA) is known to be the major component and the ratio of these isomers depends on reaction conditions and starting materials [2].

This paper concerns the elucidation of the crystal structure of PR209 so as to clarify the yellowish component in PR209 in accordance with our previous work on molecular arrangement [3–8].

2. Experimental

2.1. Materials and crystal growth

PR209 was obtained from Dainippon Ink and Chemicals, Inc and was purified by sublimation, using a two-zone furnace [9]. Single crystals were grown from the vapour phase at 743 K and, after 24 h, a number of red needle-shaped single crystals were obtained.

2.2. Equipment and measurements

Both diffuse reflectance spectra and spectra in dimethyl sulfoxide (DMSO) were recorded on a UV-2400PC spectrophotometer (Shimadzu), the former measurements were recorded using an ISR-240A integrating sphere attachment. The reflectance spectra of single crystals were measured using a UMSP80 microscope–spectrophotometer (Carl Zeiss); an Epiplan Pol (×8) objective was used together with a Nicol-type polarizer. Reflectivities were corrected relative to the reflectance standard of silicon carbide.

* Corresponding author. Tel./fax: +81 45 339 4320.
E-mail address: tsenju@ynu.ac.jp (T. Senju).

0143-7208/$ - see front matter © 2007 Elsevier Ltd. All rights reserved.
doi:10.1016/j.dyepig.2007.01.021

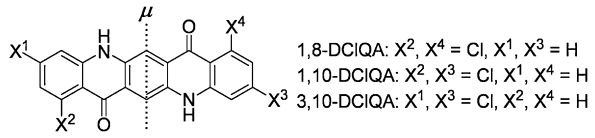

Fig. 1. Molecular structure of 3,10-DClQA. The dotted line denotes the transition dipole (μ) as deduced from MO calculations.

2.3. Molecular orbital calculations

Geometry optimization was carried out using the density functional method with B3LYP hybrid functional [10,11] together with 6-311+G(d,p) basis set using the Gaussian 03 suite of programs [12]. Absorption bands were calculated based on the time dependent density functional theory (TD-DFT) using the 6-311+G(d,p) basis set in combination with the polarizable continuum model (PCM) of Tomasi et al. [13] to include solvent effects. With regard to a larger basis set, neither an additional diffuse function on hydrogen atoms nor a larger polarization function was effective.

3. Results and discussion

3.1. Crystal structure of 3,10-DClQA

While single crystals were obtained by sublimation of PR209, which is composed of 3,10-, 1,8-, and 1,10-derivatives, the crystals were found to be 3,10-DClQA. Table 1 shows the crystallographic parameters [14]. Fig. 3 shows the ORTEP plot of the molecule from which it is apparent that the molecule has inversion symmetry. The quinacridone skeleton is entirely planar as indicated by the root mean square deviation of *ca.* 0.02 Å from the least-squares plane of the rings defined by atoms C1–C10 and N1. However, the carbonyl O atom deviates slightly (0.140(3) Å) from the QA skeleton towards the NH group of the neighbouring molecule, probably due to the formation of the NH···O intermolecular hydrogen bond. This tendency is also found in the red phase of 2,9-dichloroquinacridone [15] and 2,9-dimethylquinacridone [16].

As shown in Fig. 4(a), NH···O intermolecular hydrogen bonds lie in the [1$\bar{1}$0] direction in which one molecule is bound to two neighbouring molecules through four hydrogen bonds. The H/O and N/O distances in the hydrogen bond were 2.12 Å and 2.873(4) Å, respectively, and the angle formed by the N, H, and O atoms was 159.4°. This suggests that the NH···O hydrogen bond is quite strong; furthermore, there is a small step of *ca.* 0.55 Å between the two molecular planes of the hydrogen-bonded molecules as shown in Fig. 4(b). These

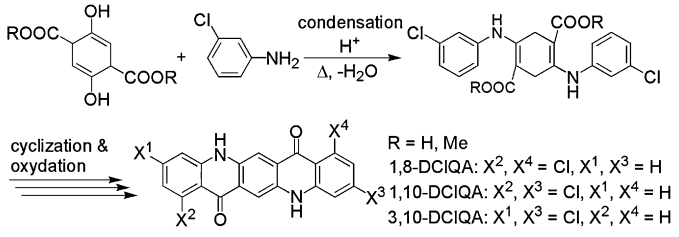

Fig. 2. Reaction scheme for the preparation of 3,10-DClQA.

Table 1
Crystallographic parameters of 3,10-DClQA

Molecular formula	$C_{20}H_{10}Cl_2N_2O_2$
Molecular weight	381.20
Crystal system	Triclinic
Space group	$P\bar{1}$
Z	1
a (Å)	3.7635(13)
b (Å)	5.853(2)
c (Å)	16.746(6)
α (°)	85.20(2)
β (°)	83.79(2)
γ (°)	89.32(2)
V (Å^3)	365.4(2)
R_1	0.057
D_{calcd} (Mg m^{-3})	1.732
T (K)	93(1)

features are quite similar to those observed for the red phase of 2,9-dichloroquinacridone [15] and 2,9-dimethylquinacridone [16].

3.2. Characterization of PR209 in solution

Table 2 shows the calculated absorption bands and oscillator strengths for 1,8-, 1,10-, and 3,10-DClQAs in DMSO; all bands can be attributed to HOMO/LUMO π–π* transitions. The direction of the transition dipole is perpendicular to the long-molecular axis as shown in Fig. 1. The absorption bands appear at about 508 nm for 1,8-DClQA, 502 nm for 1,10-DClQA, and 497 nm for 3,10-DClQA, respectively, suggesting that all the isomers have nearly the same solution spectra. Indeed, the calculated bands agree well with the solution spectrum of PR209 in DMSO shown in Fig. 5.

Fig. 5 shows the solution spectrum of PR209 in DMSO. A progression of the absorption bands was observed, starting at *ca.* 523 nm towards shorter wavelengths. Furthermore, the absorption edge of the longest-wavelength band was quite steep and all bands were almost equally spaced. This indicates that a single electronic transition is coupled with vibrational transitions and that the absorption bands can be accordingly assigned to the 0–0, 0–1, and 0–2 bands as designated in Fig. 5.

3.3. Characterization of 3,10-DClQA in single crystals

3.3.1. Polarized reflection spectra measured on single crystals

Fig. 6 shows the polarized reflection spectra measured in the (001) plane of single crystals of 3,10-DClQA together

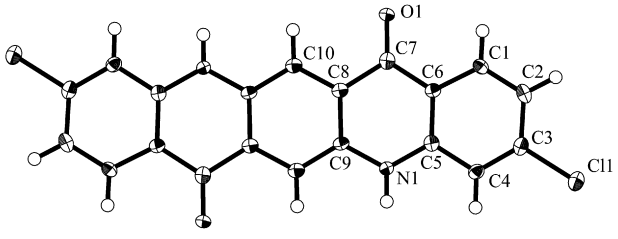

Fig. 3. ORTEP plot for the molecule of 3,10-DClQA.

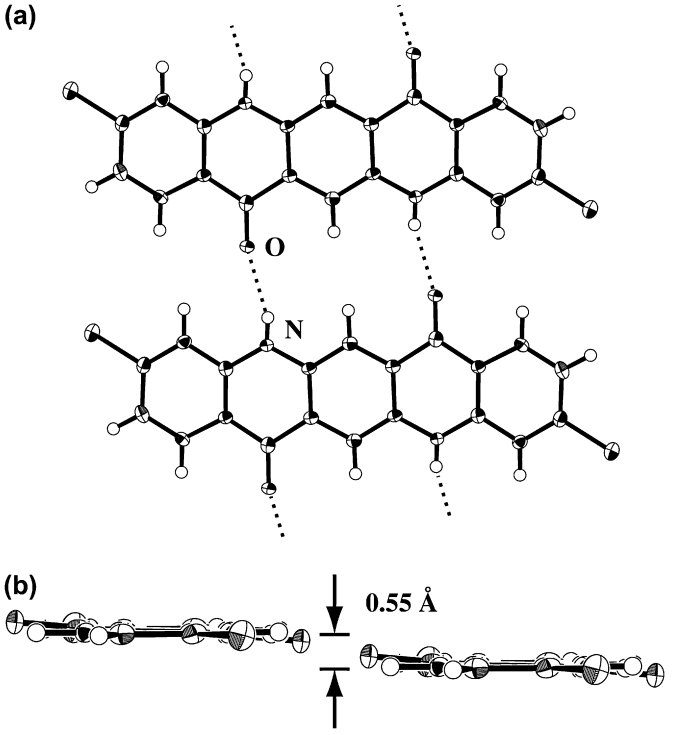

Fig. 4. (a) Top view of the two hydrogen-bonded molecules. The dotted line denotes intermolecular N–H···O hydrogen bonds and (b) side view of the two hydrogen-bonded molecules, showing a small step of *ca*. 0.55 Å.

with its projection of the crystal structure. A prominent reflection band appears around 558 nm together with two small bands around 484 and 518 nm for polarization parallel to the direction of the hydrogen bond (Fig. 6(b)). In contrast, these bands are completely quenched perpendicular to this direction. These results clearly indicate that the direction of the transition dipole points along the intermolecular hydrogen bond in accord with the direction deduced from MO calculations and that all the reflection bands belong to a single π–π* electronic transition. It is also important to note that the spectral shape in the solid state (Fig. 6(a)) is quite similar to that of the solution (Fig. 5) and the number of absorption bands is the same. Hence, one-to-one correspondence of the absorption bands between the solution and solid state spectra is possible, indicating that the molecular nature is well preserved even in the solid state and that the solid state spectrum can be pictured as a bathochromically-displaced spectrum of that in solution.

The intensity of the band around 484 nm was too small to contribute a yellowish hue to PR209, suggesting that the

Table 2
Calculated absorption bands and oscillator strength for 1,8-, 1,10-, and 3,10-DClQAs in a DMSO solution with the time dependent density functional theory at the B3LYP/6-311+G(d,p) level in combination with Tomasi's polarizable continuum model

Compound	λ_{max} (nm)	Oscillator strength (f)
1,8-DClQA	507.68	0.13
1,10-DClQA	502.27	0.12
3,10-DClQA	496.87	0.11

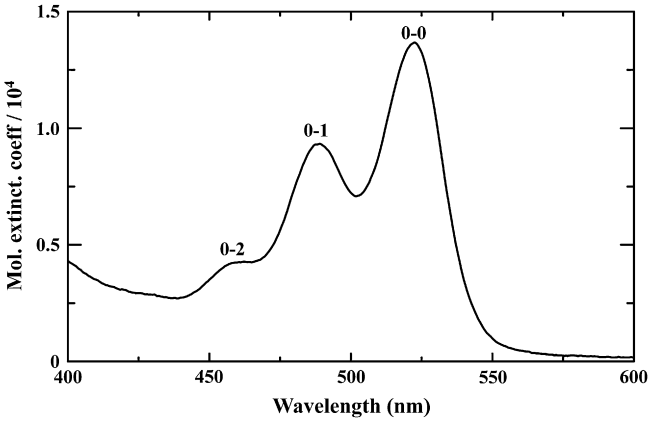

Fig. 5. Solution spectrum of PR209 in DMSO.

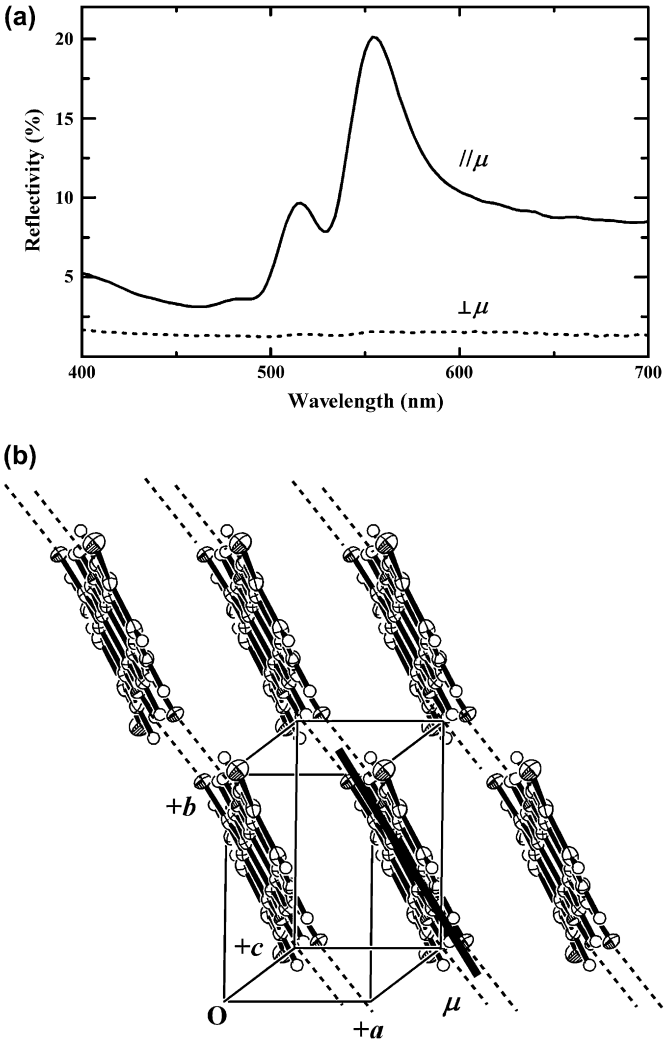

Fig. 6. (a) Polarized reflection spectra measured on the (001) plane of single crystals of 3,10-DClQA and (b) projection of the crystal structure onto the (001) plane. The thick solid line denotes the transition dipole (μ), while the intermolecular hydrogen bonds are designated by dotted lines.

pigment's characteristic yellowish red shade is due to 1,8- and 1,10-DClQA.

3.3.2. Bathochromic shift upon crystallization

Bathochromic shifts upon crystallization are often observed in QA compounds and are considered to arise from interactions between transition dipoles [3]. The NH···O intermolecular hydrogen bonds between the NH group of one molecule and the O atom of a neighbouring group align the two molecules in a "head-to-tail" fashion which imparts maximum bathochromic shift. This interaction is typical within dye and pigment systems, in which the absorption coefficient of the component molecule is high and the molecules are periodically arranged [3–8]; the outline is described below.

The interaction energy ($\Delta E_{\text{exciton}}$) is given by the dipole–dipole equation [17,18]: $\Delta E_{\text{exciton}} = |\mu|^2(1 - 3\cos^2\theta)/r^3$, where the transition dipole is denoted by μ and the distance and angle between two transition dipoles by r and θ, respectively. As is evident from this equation, the overall shift energy is determined by the strength of the interneighbour coupling ($|\mu|^2$) (i.e. is proportional to the absorption coefficient of the molecule) as well by the mutual relative orientation of the transition dipoles. In other words, the term $(1 - 3\cos^2\theta)/r^3$ determines the geometrical relationship of the transition dipoles correlated with the crystal structure. Since this term falls off as the inverse cube of distance, most of the interaction will come from nearest neighbours. The bathochromic or hypsochromic shift depends on the critical angle $\theta = 54.7°$ (i.e. $\Delta E_{\text{exciton}} = 0$), below which, the bathochromic shift will result and above which the hypsochromic shift will occur. The maximum bathochromic shift arises when the transition dipoles are arranged in a "head-to-tail" manner.

As seen from Fig. 6(b), the NH···O intermolecular hydrogen bond aligns the molecules in a near "head-to-tail" fashion (i.e. $\theta \approx 0$) which induces maximum bathochromic displacement. Furthermore, the molar extinction coefficient (which is proportional to $|\mu|^2$) of the component molecule was as high as 14 000 (Fig. 5); in addition, the center-to-center distance between two transition dipoles is relatively short (6.92 Å). Due to these parameters, a large bathochromic shift is expected to occur in 3,10-DClQA.

3.4. Characterization of PR209 in the solid state

3.4.1. Powder X-ray diffraction diagrams

Fig. 7 shows the powder X-ray diffraction diagram for PR209 and the simulated diffraction diagram of 3,10-DClQA based upon structural analysis described in Section 3.1. The two diagrams are strikingly different and only a few peaks can be assigned to 3,10-DClQA; the unassigned peaks may be attributed to other derivatives other than 3,10-DClQA or due to their solid solution.

3.4.2. Diffuse reflectance spectrum

The diffuse reflectance spectrum of powdered PR209 (Fig. 8) shows three characteristic bands in the visible region (540, 520, and 475 nm), of which the one around 520 nm

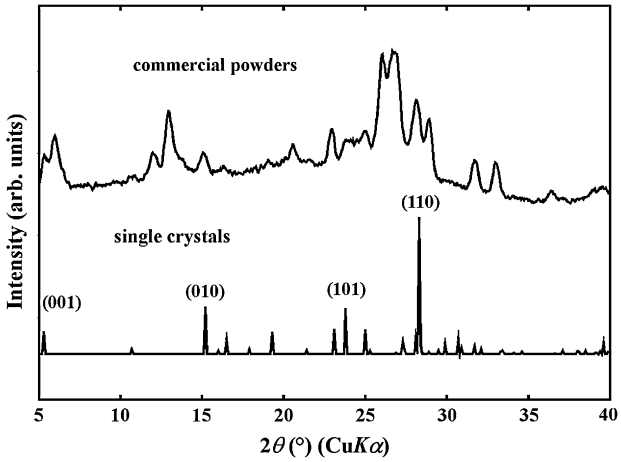

Fig. 7. X-ray diffraction diagrams: (a) powdered PR209 and (b) simulated diffraction diagram of 3,10-DClQA based upon the structure analysis.

was strongest. The absorption shoulder around 475 nm is evidently responsible for the yellowish hue of PR209. The spectral shape as well as the position and intensity of the absorption bands are appreciably different from those in the polarized reflection spectra of 3,10-DClQA (Fig. 6(a)), indicating that PR209 includes additional compounds other than 3,10-DClQA.

3.4.3. Yellowish shade in PR209

One of the appealing features of PR209 is its yellowish shade of red, which is unusual for a quinacridone pigment. The yellowish shade means that there is an absorption around 480 nm and this is clearly observed in PR209 (Fig. 8), whereas this component is missing in 3,10-DClQA (Fig. 6(a)). Furthermore, the diffraction diagram of powdered PR209 differs significantly from that of the simulated diagram based upon X-ray structural analysis of 3,10-DClQA. In this context, we propose the following explanation which may help in developing an understanding of the mechanism of the yellowish component. The discussion focuses on 1,8- and 1,10-derivatives (Fig. 1); the Cl-substituent at the 1-position in these derivatives is likely to hinder or weaken the formation of the

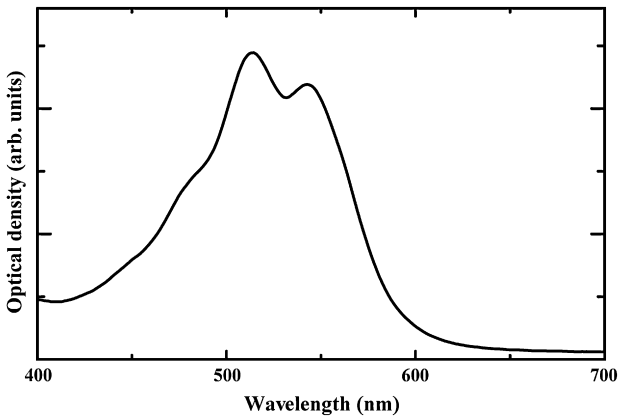

Fig. 8. Diffuse reflectance spectrum measured on powdered PR209.

NH···O hydrogen bond due to steric hindrance in comparison with that of the 3-position in 3,10-DClQA. This will profoundly influence the geometry of the hydrogen bond, which governs, directly, the extent of the bathochromic shift due to excitonic interactions. This weakening of the NH···O hydrogen bond caused by steric hindrance induces a smaller bathochromic shift compared with that of 3,10-DClQA (Fig. 6(a)). As a consequence, the complete spectrum shown in Fig. 6(a) is displaced towards shorter wavelengths, for example, by about 20 nm so that the longest-wavelength band occurs around 520 nm. The superposition of this displaced spectrum (assumed for 1,8- and 1,10-derivatives) and the spectrum of 3,10-DClQA (Fig. 6(a)) gives approximately Fig. 8. The band around 480 nm is due to the second-strongest band of the assumed spectrum of 1,8- and 1,10-derivatives.

4. Conclusions

The electronic structure of PR209 has been investigated on the basis of its crystal structure. Single crystals of 3,10-DClQA were isolated when PR209 was sublimed under vacuum. 3,10-DClQA is found to crystallize in the $P\bar{1}$ space group and chains of NH···O hydrogen bonds lie in the [110] direction, constituting a two-dimensional network. A large bathochromic shift of 3,10-DClQA was observed upon crystallization. This can be considered to arise from interactions between transition dipoles arranged in an almost ''head-to-tail'' fashion due to the NH···O hydrogen bonds. 3,10-DClQA was found to lack absorption around 480 nm that lends a yellowish red color to PR209. This component is presumably provided by 1,8- and 1,10-DClQAs whose absorption bands appear at shorter wavelengths than those of 3,10-DClQA due to weakening of the NH···O hydrogen bonds caused by steric hindrance of the Cl-substituent located at the 1-position of the 1,8- and 1,10-derivatives.

Acknowledgements

We thank Research Center for Computational Science, Okazaki Research Facilities, National Institute of Natural Sciences for the use of Fujitsu PRIMEQUEST for the calculations.

References

[1] Herbst W, Hunger K. Industrial organic pigments. 2nd ed. VCH, Germany: Weinheim; 1997. p. 454–74.
[2] Altiparmakian RH, Bohler H, Kaul BL, Kehrer F. Quinacridones. Structure and mechanism of formation. Helv Chim Acta 1972;55(1):85–100.
[3] Mizuguchi J, Senju T. Solution and solid-state spectra of quinacridone derivatives as viewed from the intermolecular hydrogen bond. J Phys Chem B 2006;110(39):19154–61.
[4] Mizuguchi J, Shikamori H. Spectral and crystallographic coincidence in a mixed crystal of two components and a crystal of their hybrid component in pyrrolopyrrole pigments. J Phys Chem B 2004;108(7):2154–61.
[5] Senju T, Mizuguchi J. Electronic structure of thiazine-indigo pigment on the basis of the crystal structure. J Phys Chem B 2005;109(16):7649–53.
[6] Mizuguchi J, Tojo K. Electronic structure of perylene pigments as viewed from the crystal structure and excitonic interactions. J Phys Chem B 2002;106(4):767–72.
[7] Mizuguchi J. Crystal structure and electronic characterization of *trans* and *cis* perinone pigments. J Phys Chem B 2004;108(26):8926–30.
[8] Endo A, Matsumoto S, Mizuguchi J. Interpretation of the near-IR absorption of magnesium phthalocyanine complexes in terms of molecular distortion and exciton coupling effects. J Phys Chem A 1999;103:8193–9.
[9] Mizuguchi J. An improved method for purification of β-copper phthalocyanine. Krist Tech 1981;16:695–700.
[10] Becke AD. Density-functional thermochemistry. III. The role of exact exchange. J Chem Phys 1993;98(7):5648–52.
[11] Lee C, Yang W, Parr R. Development of the Colle–Salvetti correlation-energy formula into a functional of the electron density. Phys Rev B 1988;37(2):785–9.
[12] Gaussian 03, revision D.01. Gaussian, Inc.; 2004.
[13] Tomasi J, Mennucci B, Cammi R. Quantum mechanical continuum solvation models. Chem Rev 2005;105:2999–3094.
[14] Senju T, Hoki T, Mizuguchi J. 3,10-Dichloro-5,12-dihydroquino[2,3-*b*]acridine-7,14-dione. Acta Crystallogr 2006;E62(1):o261–3.
[15] Senju T, Nishimura N, Hoki T, Mizuguchi J. 2,9-Dichloro-5,12-dihydroquino[2,3-*b*]acridine-7,14-dione (red phase). Acta Crystallogr 2005; E61(8):o2596–8.
[16] Mizuguchi J, Senju T, Sakai M. Crystal structure of 5,12-dihydro-2,9-dimethylquino[2,3-*b*]acridine-7,14-dione. Z Krist New Cryst Struct 2002;217:525–6.
[17] Kasha M. Molecular excitons in small aggregates. In: Bartolo BD, editor. NATO ASI Ser B, vol. 12. New York: Plenum Press; 1976. p. 337–63.
[18] Craig DP, Walmsley SH. Excitons in molecular crystals: theory and applications. New York: W.A. Benjamin, Inc.; 1968.